Coupled rearrangement channel calculation of the fine and hyperfine structures of the antiprotonic helium atom

Nobuhiro Yamanaka,[1,*] Yasushi Kino,[2,3,†] Hiroshi Kudo,[2] and Masayasu Kamimura[4]
[1]*Department of Physics, University of Tokyo, Tokyo 113-0033, Japan*
[2]*Department of Chemistry, Tohoku University, Sendai 980-8578, Japan*
[3]*Department of Quantum Chemistry, Uppsala University, Box 518, 75120 Uppsala, Sweden*
[4]*Department of Physics, Kyushu University, Fukuoka 812-8581, Japan*
(Received 1 July 2000; published 13 December 2000)

We precisely calculate the fine and hyperfine structure splittings of the $(v,J)=(1,35)$ state in the antiprotonic helium atom, where v is the vibrational quantum number and J is the total orbital angular momentum. The coupled rearrangement channel method is employed to efficiently describe correlation effects in the three-body system with atomic and molecular characters. An accuracy of better than $\alpha^2 \approx 50$ ppm has been achieved. The result obtained is in good agreement with the previous calculation within ~200 ppm. We also examine the correlation effects, in particular orbital polarization effects.

DOI: 10.1103/PhysRevA.63.012518 PACS number(s): 36.10.−k, 31.30.Gs, 31.30.Jv

I. INTRODUCTION

The antiprotonic helium atom, which consists of a helium nucleus, an electron, and an antiproton, has metastable states with an extremely long lifetime of the order of a microsecond [1,2]. Such a long-lived antiprotonic atom has stimulated spectroscopic studies from the viewpoints of antimatter science: tests of CPT invariance and the weak equivalence principle, interaction between matter and antimatter, etc. (see, for example, Refs. [3–5]).

A doublet structure has been observed for the antiprotonic helium atom in the laser-induced transition with a wavelength of 726.095(4) nm between the $(v,J)=(1,35)$ and (3,34) states [6], where v is the vibrational quantum number and J is the total orbital angular momentum. This structure is caused by the interaction that depends on the electronic spin, i.e., the fine structure. Recently, a laser and microwave triple-resonance technique has been developed to resolve further the hyperfine structure, which is caused by the interaction with antiprotonic spin [7]. The precise measurement with this technique, which is in progress at the Antiproton Decelerator (AD) in CERN [7], is expected to provide us with information on the electromagnetic structure of an antiproton.

The magnetic moment of an antiproton was determined to be $\mu_{\bar{p}} = -2.8005(90)\mu_N$, where μ_N is the nuclear magneton, from an x-ray measurement for the antiprotonic ^{208}Pb atom [8] together with corresponding calculations [9,10]. However, the value determined is much less precise than that for the proton, $\mu_p = 2.792\,847\,337(29)\mu_N$. The large uncertainty comes from the lower resolution of the x-ray measurement. In addition, nuclear and QED effects are also a source of the uncertainty, causing a discrepancy of 0.1% between the two calculations [9,10]. These ambiguities are avoided if a light atom is used as a target. Hence the spectroscopy of the antiprotonic helium atom may improve the accuracy of the antiprotonic magnetic moment.

In the present paper, we precisely calculate the fine and hyperfine structure splittings of the (1,35) state. Bakalov and Korobov [11] have calculated them using variational wave functions with the prolate spheroidal coordinate [12–15]. Their result of the fine structure splitting agrees with the previous experiment [6] within several percent. The forthcoming experiment expounded upon in Ref. [7] is expected to be sufficiently precise to determine further the hyperfine splittings. We employ the coupled rearrangement channel (CRC) method [16], where wave functions are given by a linear combination of rearrangement channels. The CRC method is useful to extract a particular character, such as the atom and the molecule, from the antiprotonic helium atom and thus permits us accurately to incorporate correlation effects in the Coulomb three-body system. Moreover, the CRC method has advantages in speed and precision of computation, because matrix elements can be analytically calculated with the use of Gaussian basis functions. The linear independence between the basis functions is improved by introducing three rearrangement channels, thereby all of the calculations can be done in double precision without over complete problems. Transition wavelengths have been calculated with this method [17,18], and were found to be in excellent agreement with the laser-resonance experiment of Torii *et al.* [19,20] within the experimental error (~0.5 ppm). In the CRC method, we can clearly examine the correlation effects, in particular orbital polarization effects.

In the present paper, the atomic units $(e=\hbar=m_e=1)$ are used with the fine structure constant $\alpha=c^{-1}$ unless otherwise stated.

II. FINE AND HYPERFINE STRUCTURE

A. Spin-dependent interactions

Fine and hyperfine structures of energy levels in the antiprotonic helium atom are caused by spin-dependent interactions. The interactions are given by terms of α^2 [21–23],

$$U=\sum_{i\neq j}\left[U_{ij}^{(\mathrm{so})}+U_{ij}^{(\mathrm{ssc})}+U_{ij}^{(\mathrm{sst})}\right], \tag{1}$$

*Electronic address: yam@nucl.phys.u-tokyo.ac.jp
†Electronic address: kino@mail.cc.tohoku.ac.jp

where i and j label the following particles: the antiproton ($\bar{p}$), the helium nucleus ($^4He^{2+}$), and the electron (e). Here $\mathbf{r}_i$, $\mathbf{p}_i$, $\mathbf{s}_i$, m_i, z_i, and μ_i denote the position vector, momentum, spin, mass, electric charge, and magnetic moment in units $\alpha/2m_i$ of particle i ($=\bar{p}$, $^4He^{2+}$, or e). The three terms in Eq. (1) describe, respectively, the following three interactions: the spin-orbit interaction,

$$U_{ij}^{(\mathrm{so})}=-\alpha^2\left[\frac{z_i(z_j-2\mu_j)}{2m_j^2}\frac{(\mathbf{r}_{ij}\times\mathbf{p}_j)\cdot\mathbf{s}_j}{r_{ij}^3}+\frac{z_i\mu_j}{m_im_j}\frac{(\mathbf{r}_{ij}\times\mathbf{p}_i)\cdot\mathbf{s}_j}{r_{ij}^3}\right]; \tag{2}$$

the spin-spin contact interaction,

$$U_{ij}^{(\mathrm{ssc})}=-\alpha^2\frac{8\pi}{3}\frac{\mu_i\mu_j}{m_im_j}(\mathbf{s}_i\cdot\mathbf{s}_j)\delta(\mathbf{r}_{ij}); \tag{3}$$

and the spin-spin tensor interaction,

$$U_{ij}^{(\mathrm{sst})}=-\alpha^2\frac{\mu_i\mu_j}{m_im_j}\left[3\frac{(\mathbf{r}_{ij}\cdot\mathbf{s}_i)(\mathbf{r}_{ij}\cdot\mathbf{s}_j)}{r_{ij}^5}-\frac{(\mathbf{s}_i\cdot\mathbf{s}_j)}{r_{ij}^3}\right], \tag{4}$$

where $\mathbf{r}_{ij}=\mathbf{r}_i-\mathbf{r}_j$. For a spinless particle i ($^4He^{2+}$), the terms including $\mathbf{s}_i$ are dropped from Eq. (1).

Note that by using empirical values for the magnetic moment μ_i, we can incorporate the anomalous magnetic moment that contributes to the order of α^3. Higher-order effects contribute to the order of α^4. Hence the spin-dependent interaction operator (1) is accurate up to the order of α^3.

B. First-order correction

The spin-dependent interactions are very weak and hence calculated in the first-order perturbation theory. We denote by Ψ_{vJM_J} wave functions that describe relative motions of the particles, where v is the vibrational quantum number associated with radial motion between the antiproton and the helium nucleus and J is the total orbital angular momentum. The eigenfunction that describes the fine and hyperfine structures is written in a form of

$$|vJFM_F\rangle=\sum_K \beta_{vJF}^K|vJKFM_F\rangle, \tag{5}$$

where

$$|JKFM_F\rangle=\sum_{M_JM_eM_Km_{\bar{p}}} C_{JM_J,s_em_e}^{KM_K}C_{KM_K,s_{\bar{p}}m_{\bar{p}}}^{FM_F}|\Psi_{vJM_J}\rangle|s_em_e\rangle|s_{\bar{p}}m_{\bar{p}}\rangle. \tag{6}$$

Here, K is the intermediate angular momentum ($\mathbf{K}=\mathbf{J}+\mathbf{s}_e$), F is the total angular momentum ($\mathbf{F}=\mathbf{K}+\mathbf{s}_{\bar{p}}$), C is the Clebsch-Gordan coefficient, and $|sm\rangle$ is the angular-momentum state vector.

The energy-level corrections ΔE_{vJF}^K and the amplitudes β_{vJF}^K are determined by diagonalizing the spin-dependent interaction matrix,

$$\sum_{K'}(\langle vJKFM_F|U|vJK'FM_F\rangle-\Delta E_{vJF}^K\delta_{KK'})\beta_{vJF}^{K'}=0. \tag{7}$$

Here, we define an effective Hamiltonian $\mathcal{U}$, which corresponds to Eq. (1) as [11]

$$(JKFM_F|\mathcal{U}|JK'FM_F)=\langle vJKFM_F|U|vJK'FM_F\rangle, \tag{8}$$

in the space $|JKFM_F)$ of the three angular-momentum coupled states,

$$|JKFM_F)=\sum_{M_JM_eM_Km_{\bar{p}}} C_{JM_J,s_em_e}^{KM_K}C_{KM_K,s_{\bar{p}}m_{\bar{p}}}^{FM_F}|JM_J\rangle|s_em_e\rangle|s_{\bar{p}}m_{\bar{p}}\rangle. \tag{9}$$

The effective Hamiltonian is given by

$$\mathcal{U}=\varepsilon_{vJ}^{(\mathrm{so};e)}(\mathbf{J}\cdot\mathbf{s}_e)+\varepsilon_{vJ}^{(\mathrm{so};\bar{p})}(\mathbf{J}\cdot\mathbf{s}_{\bar{p}})+\varepsilon_{vJ}^{(\mathrm{ssc})}(\mathbf{s}_e\cdot\mathbf{s}_{\bar{p}})+\varepsilon_{vJ}^{(\mathrm{sst})}\tilde{T}_{e\bar{p}}, \tag{10}$$

with

$$\tilde{T}_{e\bar{p}}=2J(J+1)(\mathbf{s}_e\cdot\mathbf{s}_{\bar{p}})-3[(\mathbf{J}\cdot\mathbf{s}_e)(\mathbf{J}\cdot\mathbf{s}_{\bar{p}})+(\mathbf{J}\cdot\mathbf{s}_{\bar{p}})(\mathbf{J}\cdot\mathbf{s}_e)], \tag{11}$$

where the coefficients $\varepsilon_{vJ}^{(\mathrm{so};e)}$, $\varepsilon_{vJ}^{(\mathrm{so};\bar{p})}$, $\varepsilon_{vJ}^{(\mathrm{ssc})}$, and $\varepsilon_{vJ}^{(\mathrm{sst})}$ are called the electron spin-orbit, antiproton spin-orbit, contact, and tensor parameters. The parameters are calculated from

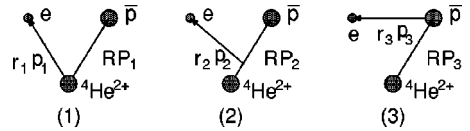

FIG. 1. Three coordinate systems corresponding to the rearrangement channels ($c=1$, 2, and 3). Channel (1) is suitable for describing the atomic character of the antiprotonic helium atom. Channel (2) is for describing the diatomic molecular character. Channel (3) is introduced to effectively describe the correlation between the electron and the antiproton. The momenta $\mathbf{p}_c$ and $\mathbf{P}_c$ are the conjugate momenta of the relative position vectors $\mathbf{r}_c$ and $\mathbf{R}$.

TABLE I. The spin-orbit, contact, and tensor parameters (a.u.) calculated with the CRC wave function given by a single channel of $c=1$ for the (1,35) state. Numbers in square brackets indicate powers of 10. E_{vJ} is the eigenvalue (a.u.).

$l_{\max}$	$\varepsilon_{vJ}^{(\mathrm{so};e)}$	$\varepsilon_{vJ}^{(\mathrm{so},\bar{p})}$	$\varepsilon_{vJ}^{(\mathrm{ssc})}$	$\varepsilon_{vJ}^{(\mathrm{sst})}$	E_{vJ}
0	−0.388 313[−7]	0.720 486[−9]	−0.126 005[−6]	−0.902 269[−11]	−2.830 991 76
1	−0.549 358[−7]	0.642 074[−9]	−0.704 151[−7]	−0.999 680[−11]	−2.894 571 03
2	−0.556 455[−7]	0.639 348[−9]	−0.616 249[−7]	−0.995 909[−11]	−2.897 886 74
3	−0.565 522[−7]	0.635 177[−9]	−0.588 407[−7]	−0.991 079[−11]	−2.898 459 22
4	−0.568 880[−7]	0.633 988[−9]	−0.574 503[−7]	−0.988 444[−11]	−2.898 663 19

$$\varepsilon_{vJ}^{(\mathrm{so};e)}=\frac{\langle vJKF\|U_{\bar{p}e}^{(\mathrm{so})}+U_{\mathrm{He},e}^{(\mathrm{so})}\|vJK'F\rangle}{(JKF\|\mathbf{J}\cdot\mathbf{s}_e\|JK'F)}, \tag{12}$$

$$\varepsilon_{vJ}^{(\mathrm{so};\bar{p})}=\frac{\langle vJKF\|U_{\mathrm{He}\bar{p}}^{(\mathrm{so})}+U_{e\bar{p}}^{(\mathrm{so})}\|vJK'F\rangle}{(JKF\|\mathbf{J}\cdot\mathbf{s}_{\bar{p}}\|JK'F)}, \tag{13}$$

$$\varepsilon_{vJ}^{(\mathrm{ssc})}=\frac{\langle vJKF\|U_{e\bar{p}}^{(\mathrm{ssc})}\|vJK'F\rangle}{(JKF\|\mathbf{s}_e\cdot\mathbf{s}_{\bar{p}}\|JK'F)}, \tag{14}$$

and

$$\varepsilon_{vJ}^{(\mathrm{sst})}=\frac{\langle vJKF\|U_{e\bar{p}}^{(\mathrm{sst})}\|vJK'F\rangle}{(JKF\|\tilde{T}_{e\bar{p}}\|JK'F)}, \tag{15}$$

III. CRC WAVE FUNCTIONS AND NUMERICAL METHOD

In the CRC method, to accurately include correlation effects, we introduce three rearrangement channels ($c=1$, 2, and 3) corresponding, respectively, to three coordinate systems [17,18] illustrated in Fig. 1. Channel (1) is suitable for describing the atomic character. Channel (2) is for describing the diatomic molecular character. Channel (3) is introduced to effectively describe correlation between the electron and the antiproton. As shown in Fig. 1, we denote by $\mathbf{r}_c$ and $\mathbf{R}=\mathbf{r}_{\bar{p}}-\mathbf{r}_{\mathrm{He}}$ the relative position vectors,

$$\begin{pmatrix}\mathbf{r}_1\\ \mathbf{r}_2\\ \mathbf{r}_3\end{pmatrix}=\begin{pmatrix}0 & -1 & 1\\ -\dfrac{m_{\bar{p}}}{m_{\bar{p}}+m_{\mathrm{He}}} & -\dfrac{m_{\mathrm{He}}}{m_{\bar{p}}+m_{\mathrm{He}}} & 1\\ -1 & 0 & 1\end{pmatrix}\begin{pmatrix}\mathbf{r}_{\bar{p}}\\ \mathbf{r}_{\mathrm{He}}\\ \mathbf{r}_e\end{pmatrix}. \tag{16}$$

The momentum $\mathbf{p}_i$ of the particle i is rewritten with the conjugate momenta $\mathbf{p}_c$ and $\mathbf{P}_c$ of $\mathbf{r}_c$ and $\mathbf{R}$,

$$\begin{pmatrix}\mathbf{p}_{\bar{p}}\\ \mathbf{p}_{\mathrm{He}}\\ \mathbf{p}_e\end{pmatrix}=\begin{pmatrix}0 & 1\\ -1 & -1\\ 1 & 0\end{pmatrix}\begin{pmatrix}\mathbf{p}_1\\ \mathbf{P}_1\end{pmatrix}=\begin{pmatrix}-\dfrac{m_{\bar{p}}}{m_{\bar{p}}+m_{\mathrm{He}}} & 1\\ -\dfrac{m_{\mathrm{He}}}{m_{\bar{p}}+m_{\mathrm{He}}} & -1\\ 1 & 0\end{pmatrix}\begin{pmatrix}\mathbf{p}_2\\ \mathbf{P}_2\end{pmatrix}$$
$$=\begin{pmatrix}-1 & 1\\ 0 & -1\\ 1 & 0\end{pmatrix}\begin{pmatrix}\mathbf{p}_3\\ \mathbf{P}_3\end{pmatrix}. \tag{17}$$

The CRC wave function is defined by a sum of channel wave functions $\Phi_{vJM_J}^{(c)}$,

$$\Psi_{vJM_J}=\sum_{c=1}^{3}\Phi_{vJM_J}^{(c)}(\mathbf{r}_c,\mathbf{R}). \tag{18}$$

Each channel function is given by a linear combination of configuration state functions (CSF's) $\phi_{vJM_J}^{(c)l_cL_c}$ with the same vibrational quantum number (v) and total orbital angular momentum (J),

TABLE II. The spin-orbit, contact, and tensor parameters (a.u.) calculated with the CRC wave function given by double channels of $c=1$ and 2 for the (1,35) state. The notations are the same as in Table I.

$l_{\max}$	$\varepsilon_{vJ}^{(\mathrm{so};e)}$	$\varepsilon_{vJ}^{(\mathrm{so},\bar{p})}$	$\varepsilon_{vJ}^{(\mathrm{ssc})}$	$\varepsilon_{vJ}^{(\mathrm{sst})}$	E_{vJ}
0	−0.535 910[−7]	0.693 980[−9]	−0.661 674[−7]	−0.992 615[−11]	−2.896 273 01
1	−0.551 326[−7]	0.640 550[−9]	−0.560 326[−7]	−0.989 870[−11]	−2.898 889 93
2	−0.554 567[−7]	0.639 572[−9]	−0.538 934[−7]	−0.987 524[−11]	−2.899 080 92
3	−0.557 835[−7]	0.638 433[−9]	−0.532 444[−7]	−0.986 544[−11]	−2.889 123 66
4	−0.557 603[−7]	0.638 488[−9]	−0.532 047[−7]	−0.986 229[−11]	−2.899 128 83

TABLE III. The spin-orbit, contact, and tensor parameters (a.u.) calculated with the CRC wave function given by three channels of $c=1$, 2, and 3 for the (1,35) state. The notations are the same as in Table I.

$l_{\max}$	$\varepsilon_{vJ}^{(\mathrm{so};e)}$	$\varepsilon_{vJ}^{(\mathrm{so},\bar{p})}$	$\varepsilon_{vJ}^{(\mathrm{ssc})}$	$\varepsilon_{vJ}^{(\mathrm{sst})}$	E_{vJ}
0	−0.534 730[−7]	0.692 314[−9]	−0.453 013[−7]	−0.979 357[−11]	−2.898 698 17
1	−0.552 648[−7]	0.640 122[−9]	−0.451 438[−7]	−0.980 401[−11]	−2.899 281 94
2	−0.552 631[−7]	0.640 123[−9]	−0.451 436[−7]	−0.979 820[−11]	−2.899 282 15
3	−0.552 632[−7]	0.640 123[−9]	−0.451 437[−7]	−0.979 816[−11]	−2.899 282 17
4	−0.552 632[−7]	0.640 123[−9]	−0.451 436[−7]	−0.979 816[−11]	−2.899 282 17
Ref. [11]	−0.552 519[−7]	0.640 123[−9]	−0.451 341[−7]	−0.979 852[−11]	−2.899 282 14

$$\Phi_{vJM_J}^{(c)}(\mathbf{r}_c,\mathbf{R})=\sum_{l_c,L_c}\phi_{vJM_J}^{(c)l_cL_c}(\mathbf{r}_c,\mathbf{R}). \tag{19}$$

Each CSF is given by a sum of Gaussian basis functions [16],

$$\phi_{vJM_J}^{(c)l_cL_c}(\mathbf{r}_c,\mathbf{R})=\sum_{n,N}A_{v,nl_cNL_c}^{(c)}r_c^{l_c}R^{L_c}e^{-(r_c/r_n)^2}\times e^{-(R/R_N)^2}\sum_{mM}C_{l_cm,L_cM}^{JM_J}Y_{l_cm}(\hat{\mathbf{r}}_c)Y_{L_cM}(\hat{\mathbf{R}}), \tag{20}$$

where Y_{lm} is the spherical harmonics, and l_c and L_c are the orbital angular momenta of relative motion associated with the coordinates $\mathbf{r}_c$ and $\mathbf{R}$. The Gaussian range parameters r_n and R_N are given according to the geometrical progression [16] to describe both short-range correlations and long-range tail behavior [17,24] as

$$r_n=r_{\min}a^{n-1}\quad(n=1\sim n_{\max}), \tag{21}$$

$$R_N=R_{\min}A^{N-1}\quad(N=1\sim N_{\max}), \tag{22}$$

where $a=(r_{\max}/r_{\min})^{1(n_{\max}-1)}$ and $A=(R_{\max}/R_{\min})^{1/(N_{\max}-1)}$. The coefficients $A_{v,nl_cNL_c}^{(c)}$ have been obtained with the Rayleigh-Ritz variational method in Refs. [17,18].

In the present calculation, the antiprotonic magnetic moment is taken to be the opposite sign of the protonic magnetic moment, $\mu_{\bar{p}}=-2.792\,85\mu_N$. The interaction matrix elements in Eqs. (12)–(15) are calculated with the transformation among the rearrangement channel coordinates [16]. The interaction operators (2), (3), and (4) include r_{ij}^{-3} or $\delta(r_{ij})$. The operators are rewritten with the relative position vectors and the conjugate momenta by taking a rearrangement channel that includes r_{ij} as an intrinsic coordinate, e.g., channel (3) for the contact and tensor parameters. Accordingly, channel wave functions are rewritten with coordinates in the rearrangement channel. As a result, the interaction matrix element is analytically calculated.

The fine and hyperfine structures are sensitive to correlation effects, in particular polarization effects of electronic and antiprotonic orbits. To describe efficiently the orbital polarization in Eq. (19), the channel wave function is expanded as

$$\Phi_{vJM_J}^{(c)}(\mathbf{r}_c,\mathbf{R})=\sum_{l_c=0}^{l_{\max}}\sum_{L_c=J-l_c}^{J+l_c}\phi_{vJM_J}^{(c)l_cL_c}(\mathbf{r}_c,\mathbf{R}), \tag{23}$$

where $l_{\max}$ is the upper limit of l_c, indicating the order of approximation. In the zeroth-order approximation ($l_{\max}=0$), the channel function is given by a CSF corresponding to the reference configuration $(l_c,L_c)=(0,J)$, where the electron is in an s state. In the first-order approximation ($l_{\max}=1$), CSF's corresponding to the configurations $(1,J+1)$ and $(1,J-1)$ are incorporated in the channel function. The orbital polarization is accurately incorporated by taking a sufficiently high value of $l_{\max}$. Furthermore, we construct the CRC wave functions in three ways by taking different combinations of channels: a single channel of $c=1$, double channels of $c=1$ and 2, and triple channels of $c=1$, 2, and 3. In calculations, $l_{\max}$ is taken in common among the three channels. Then we examine how the parameters converge with respect to $l_{\max}$ by increasing $l_{\max}$ up to 4.

IV. RESULTS AND DISCUSSION

A. Spin-orbit, contact, and tensor parameters

The results of calculation of the spin-orbit, contact, and tensor parameters for the (1,35) state are shown in Tables I, II, and III. For parameters listed in Table I, the CRC wave functions were generated with the single rearrangement channel of $c=1$. It is seen in Table I that all the parameters converge with the upper limit $l_{\max}$. The parameters show remarkable changes between $l_{\max}=0$ and 1. This indicates that the p-type orbital polarization is crucial in the atomic picture. Note that similar behavior was found in a calculation with the single channel of $c=2$. The convergence was slightly better than that in the calculation of $c=1$. However, the convergence is slow; higher-order orbital polarization is also important.

Table II shows the parameters calculated with the CRC wave function generated with the two channels of $c=1$ and 2. The parameters seemingly converge up to ~100 ppm more rapidly than those in Table I. The changes between $l_{\max}=0$ and 1 are much smaller than those in Table I. Thus the CRC wave function with a hybrid character of an atom

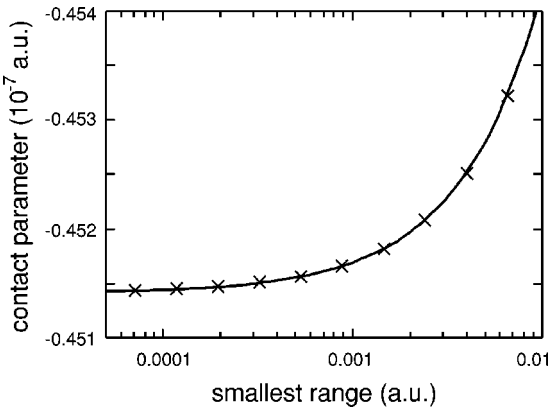

FIG. 2. Convergence of the contact parameter with respect to the smallest range $r_{\min}$ in the set of the Gaussian basis functions. The parameter is extrapolated to $-0.451\,416\times10^{-7}$ a.u. at the vanishing smallest range.

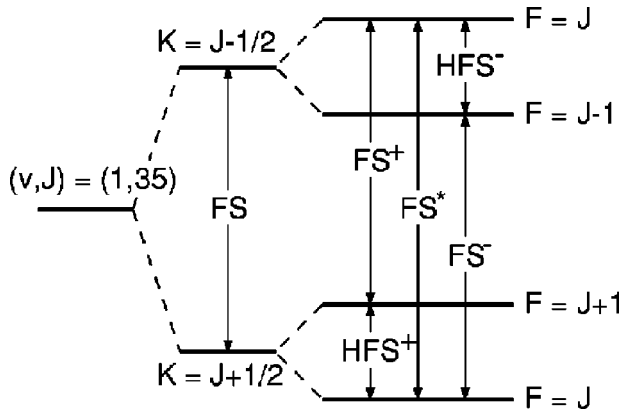

FIG. 3. Fine and hyperfine structures of the (1,35) state. FS denotes the fine structure splitting of the (1,35) state, $\mathrm{HFS}^{\pm}$ denotes the hyperfine structure splittings of the $K=J\pm\frac{1}{2}$ states, and $\mathrm{FS}^{\pm,*}$ denotes the fine and hyperfine splittings of the $F=J\pm1,J$ states.

and a molecule is found to efficiently incorporate orbital polarization.

Table III shows the parameters calculated with the CRC wave function generated with all of the three channels of $c=1$, 2, and 3. The convergence has been drastically improved, being better than 1 ppm; the parameters almost converge already at $l_{\max}=1$. This fact indicates that the higher-order orbital polarization has been accurately described by the CRC wave function. Among the four parameters, the contact parameter is most sensitive to the orbital polarization. The contact parameter in Table III remarkably deviates from that in Tables I and II, while good agreement is seen for the other parameters.

Noting this point, we confirm convergence of the contact parameter as follows. Since the contact parameter is determined by electron density at the origin of the antiproton, we examine the convergence of the parameter with respect to the smallest range in the set of the Gaussian basis functions used for generating the CRC wave functions. Figure 2 shows the behavior of this convergence for $l_{\max}=4$ in Table III. Here the parameter is calculated for respective basis sets characterized by the smallest range; the basis functions are taken in such a way that the smallest range, $r_{\min}$, is decreased with the number of basis functions, while the largest range, $r_{\max}$, is left fixed, and relation (21) is among the ranges retained. The convergence is clearly seen in the figure; the contact parameter is extrapolated to $-0.451\,416\times10^{-7}$ a.u. at the vanishing smallest range.

In Table III, the antiproton spin-orbit and tensor parameters are in good agreement with the previous result [11], while the electron spin orbit and contact parameters slightly deviate ($\sim$200 ppm) from the previous values. We conclude that the present calculation is more accurate than the previous calculation [11] from the following observations. First, the convergence of better than 1 ppm has been achieved in the present calculation, while that in the previous calculation is reported to be of order 10 ppm. Second, the wave function used in the present calculation is expected to be more accurate than that in Ref. [11], because the eigenvalue E_{vJ} obtained is lower. We should note that, in relation to the second point, the effect of couplings with Auger-decay channels is negligible; for the (1,35) state, the Auger width is as small as $\sim10^{-16}$ a.u. [25]. The accuracy of the present calculation is better than the uncertainty ($\sim\alpha^2$) of the spin-dependent interaction operators.

B. Fine and hyperfine splittings

Table IV lists the fine and hyperfine splittings of the (1,35) state. The notations are shown in Fig. 3; FS denotes the fine structure splitting of the (1,35) state, $\mathrm{HFS}^{\pm}$ denotes the hyperfine structure splittings of the $K=J\pm\frac{1}{2}$ states, and $\mathrm{FS}^{\pm,*}$ denotes the fine and hyperfine splittings of the $F=J\pm1,J$ states. The splittings have been calculated with the values in Table III for the electron spin orbit, antiproton spin orbit, and tensor parameters, and the extrapolated value of the contact parameter in Fig. 2. All the splittings obtained are in good agreement with the previous result [11]. The discrepancy ($\sim$200 ppm) in the FS's arises from that in the electron spin-orbit parameter, while the discrepancy ($\sim$200 ppm) in the HFS's arises from that in the contact parameter. Note that the discrepancy in the HFS's caused by the interaction with the antiprotonic spin is one digit lower than the precision (0.3%) of the current value of the antiprotonic magnetic moment.

TABLE IV. Fine and hyperfine splittings (GHz) of the (1,35) state in the antiprotonic helium atom. The notations are shown in Fig. 3.

	Present work	Ref. [11]
FS	12.908 648	12.906 011
FS^+	12.898 977	12.896 310
FS^-	12.926 884	12.924 278
FS*	13.059 871	13.057 234
HFS^+	0.132 987	0.132 956
HFS^-	0.160 894	0.160 924

V. CONCLUSION

We have calculated the fine and hyperfine splittings of the (1,35) state in the antiprotonic helium atom. The accuracy of better than $\alpha^2 \approx 50$ ppm has been achieved. The result is in good agreement with the previous result within ~ 200 ppm. We have also examined the correlation effects, in particular orbital polarization effects, through the convergence in the configuration expansion. For the single channel, the *p*-type orbital polarization is crucial for the fine and hyperfine structures. By introducing all of the three rearrangement channels, the orbital polarization has been sufficiently incorporated. As a result, the convergence has been drastically improved, being better than 1 ppm.

ACKNOWLEDGMENTS

We are grateful to Dr. D. Bakalov and Dr. V. I. Korobov for helpful discussions. We are particularly indebted to Dr. R. S. Hayano, Dr. E. Widmann, Dr. T. Ishikawa, Dr. T. Yamazaki, Dr. H. A. Torii, Dr. M. Hori, and Dr. A. Ichimura for many valuable suggestions. N. Y. acknowledges support from the Japan Society for the Promotion of Science. Y. K. wishes to acknowledge the Grant-in-Aid for Scientific Research, Ministry of Education and Culture, and Inoue Foundation for Science for generous financial support. The computations were carried out on the FA-COM/VPP700E at RIKEN and FACOM/VPP500 at JAERI.

[1] M. Iwasaki, S. N. Nakamura, K. Shigaki, Y. Shimizu, H. Tanuma, T. Ishikawa, R. S. Hayano, E. Takada, E. Widmann, H. Outa, M. Aoki, P. Kitching, and T. Yamazaki, Phys. Rev. Lett. **67**, 1246 (1991).

[2] T. Yamazaki, E. Widmann, R. S. Hayano, M. Iwasaki, S. N. Nakamura, K. Shigaki, F. J. Hartmann, H. Daniel, T. von Egidy, P. Hofmann, Y.-S. Kim, and J. Eades, Nature (London) **361**, 238 (1993).

[3] M. Charlton, J. Eades, D. Horváth, R. J. Hughes, and C. Zimmermann, Phys. Rep. **241**, 65 (1992).

[4] J. Eades and F. J. Hartmann, Rev. Mod. Phys. **71**, 373 (1999).

[5] M. H. Holzscheiter and M. Charlton, Rep. Prog. Phys. **62**, 1 (1999).

[6] E. Widmann, J. Eades, T. Yamazaki, H. A. Torii, R. S. Hayano, M. Hori, T. Ishikawa, M. Kumakura, N. Morita, I. Sugai, F. J. Hartmann, T. von Egidy, B. Ketzer, C. Maierl, P. Pohl, and D. Horváth, Phys. Lett. B **404**, 15 (1997).

[7] E. Widmann, Hyperfine Interact. **119**, 195 (1999).

[8] A. Kreissl, A. D. Hancock, H. Koch, T. Köhler, H. Poth, U. Raich, D. Rohmann, A. Wolf, L. Tauscher, A. Nilsson, M. Suffert, M. Chardalas, S. Dedoussis, H. Daniel, T. von Egidy, F. J. Hartmann, W. Kanert, H. Plendl, G. Schmidt, and J. J. Reidy, Z. Phys. C **37**, 557 (1988).

[9] E. Borie, Phys. Rev. A **28**, 555 (1983).

[10] G. Bohnert, R. Decker, H. Pilkuhn, and H. G. Schlaile, Phys. Lett. B **174**, 15 (1986).

[11] D. Bakalov and V. I. Korobov, Phys. Rev. A **57**, 1662 (1998).

[12] V. I. Korobov, Phys. Rev. A **54**, R1749 (1996).

[13] V. I. Korobov and D. Bakalov, Phys. Rev. Lett. **79**, 3379 (1997).

[14] V. I. Korobov, Hyperfine Interact. **119**, 185 (1999).

[15] V. I. Korobov, D. Bakalov, and H. J. Monkhorst, Phys. Rev. A **59**, R919 (1999).

[16] M. Kamimura, Phys. Rev. A **38**, 621 (1988).

[17] Y. Kino, M. Kamimura, and H. Kudo, Nucl. Phys. A **631**, 649c (1998).

[18] Y. Kino, M. Kamimura, and H. Kudo, Hyperfine Interact. **119**, 201 (1999).

[19] H. A. Torii, Hyperfine Interact. **119**, 213 (1999).

[20] H. A. Torii, R. S. Hayano, M. Hori, T. Ishikawa, N. Morita, M. Kumakura, I. Sugai, T. Yamazaki, B. Ketzer, F. J. Hartmann, T. von Egidy, R. Pohl, C. Maierl, D. Horváth, J. Eades, and E. Widmann, Phys. Rev. A **59**, 223 (1999).

[21] G. Breit, Phys. Rev. **34**, 553 (1929).

[22] Z. V. Chraplyvy, Phys. Rev. **91**, 388 (1953); **92**, 1310 (1953).

[23] J. Sucher and H. M. Foley, Phys. Rev. **95**, 966 (1954).

[24] Y. Kino, M. R. Harston, I. Shimamura, E. A. G. Armour, and M. Kamimura, Phys. Rev. A **52**, 870 (1995).

[25] V. I. Korobov and I. Shimamura, Phys. Rev. A **56**, 4587 (1997).